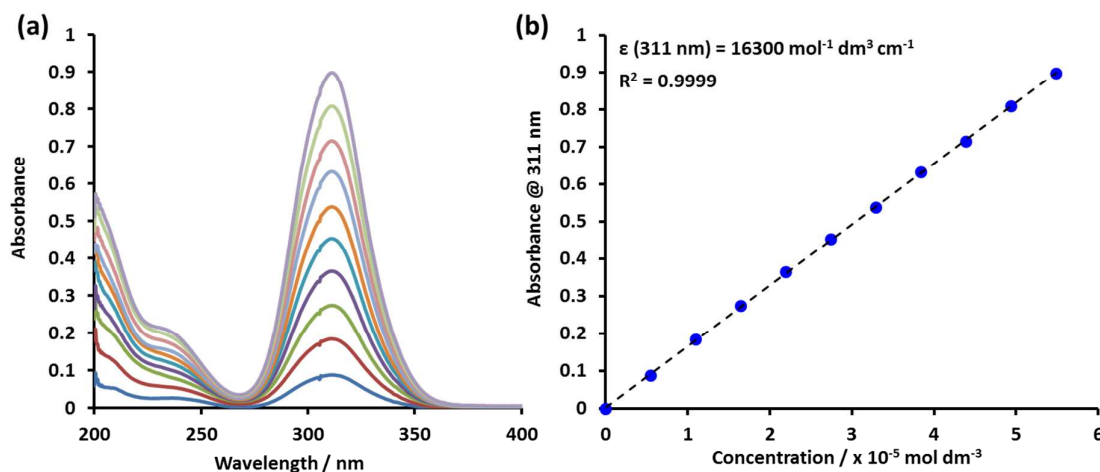# Supporting Information for:

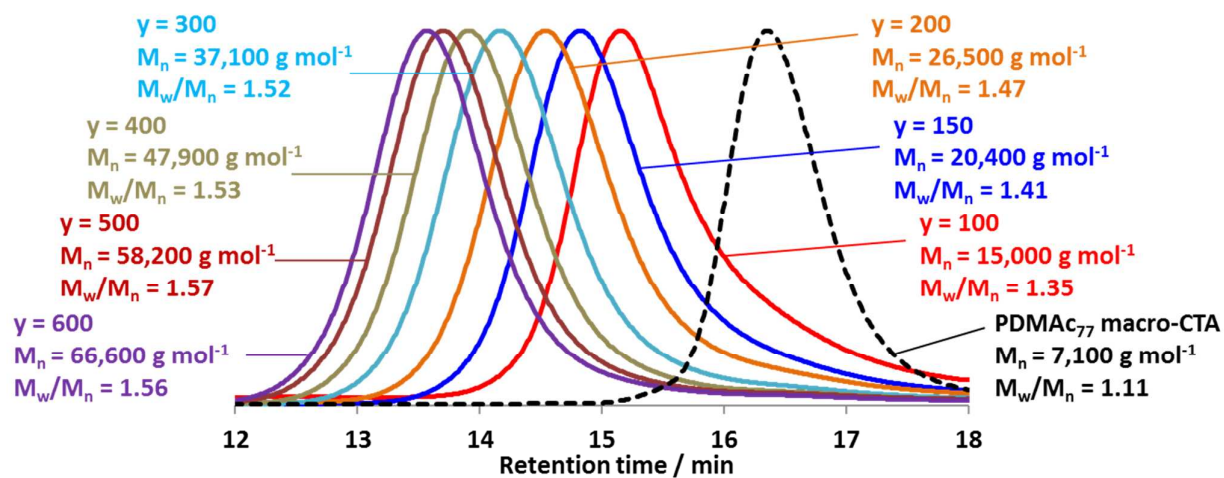## Preparation and Cross-linking of All-Acrylamide Diblock Copolymer Nano-objects via Polymerization-Induced Self-Assembly in Aqueous Solution

Sarah J. Byard, Mark Williams, Beulah E. McKenzie, Adam Blanazs and Steven P. Armes*

Figure S1. (a) UV/visible absorption spectra recorded for 2-(dodecylthiocarbonothioylthio)-2-methylpropionic acid (DDMAT) in methanol for DDMAT concentrations ranging from 5.5 μmol dm^{-3} to 54.9 μmol dm^{-3}. (b) Beer-Lambert calibration plot constructed for DDMAT in methanol to calculate the molar extinction coefficient (ε) of the absorption maximum at 311 nm.

[As pointed out by one reviewer of this manuscript, the molar extinction coefficients for the DDMAT CTA and the PDMAC-DDMAT macro-CTA may not necessarily be identical. However, in practice the wavelength maxima for these two species differ by only 2 nm (311 nm vs. 309 nm, respectively). This suggests that the corresponding molar extinction coefficients may be rather similar. To examine whether this was indeed the case, a relatively short PDMAC macro-CTA was prepared with a target DP of 15. For such low DPs, NMR spectroscopy is relatively accurate and hence can be compared to the mean DP obtained from UV spectroscopy. In both cases, the mean DP for the PDMAC-DDMAT macro-CTA was found to be 17. Thus any difference in molar extinction coefficients between the DDMAT CTA and the PDMAC-DDMAT macro-CTA is clearly negligible. Hence the mean DPs calculated using UV spectroscopy data that are reported in the main manuscript obtained for macro-CTAs with longer DPs are considered reliable.]
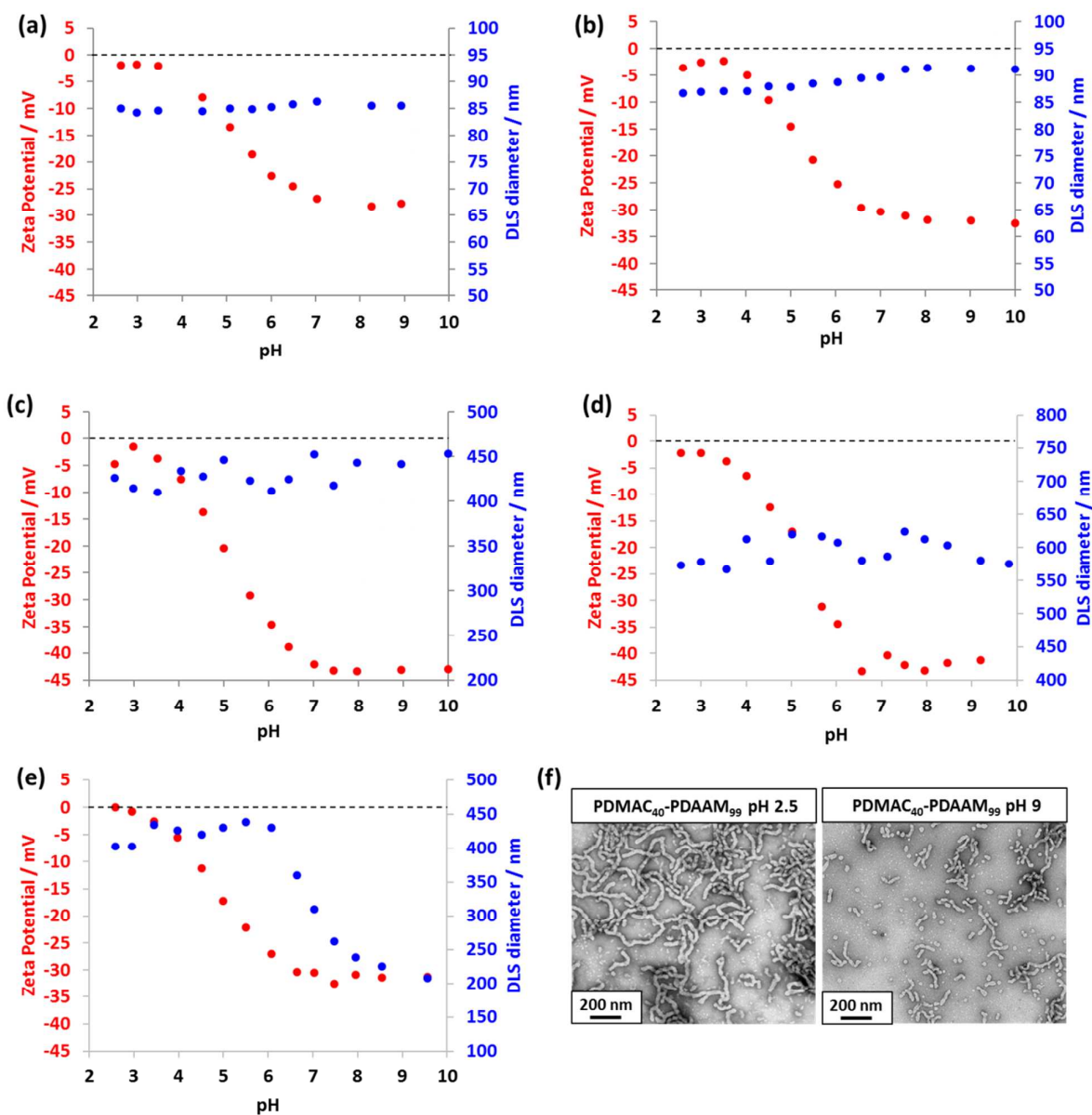
Figure S2. GPC chromatograms recorded using DMF eluent containing 10 mM LiBr with a refractive index detector for a series of PDMAC$_{77}$-PDAAM$_y$ where y = 100 to 600. Calibration against a series of ten near-monodisperse poly(methyl methacrylate) standards.
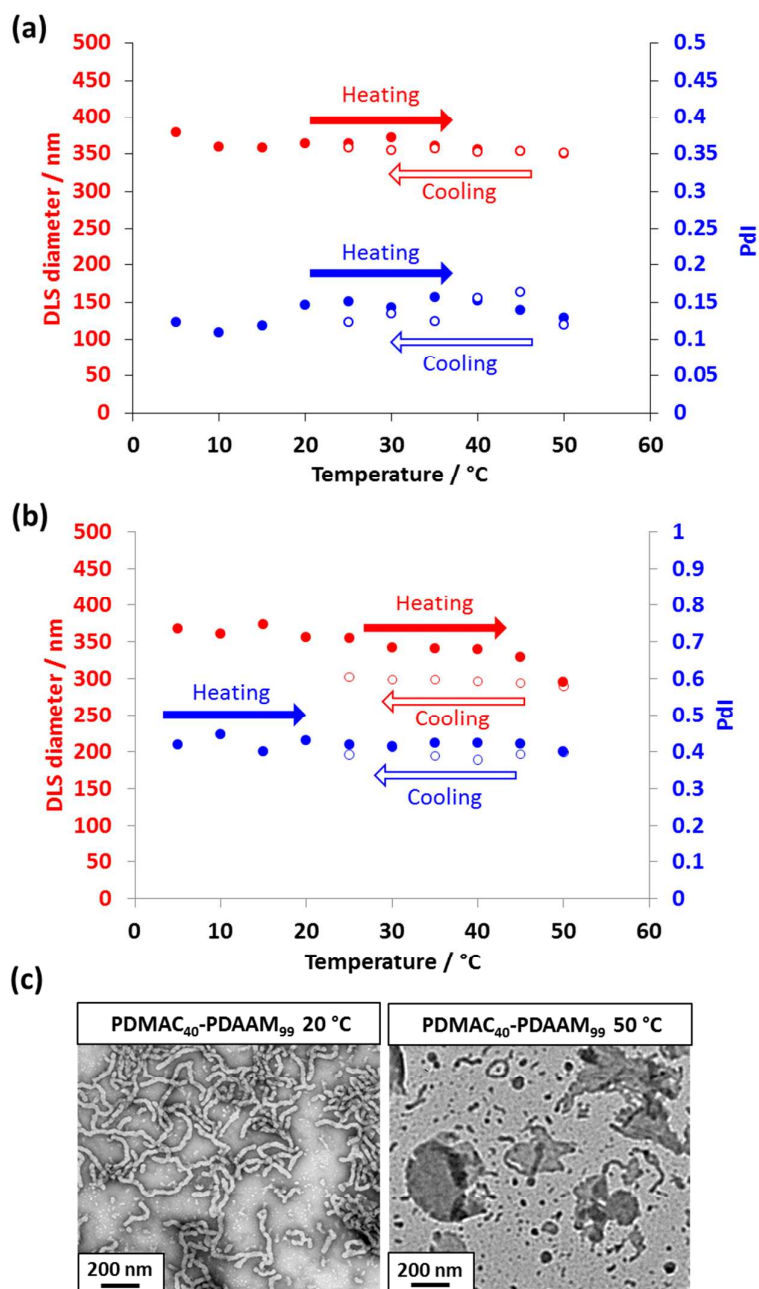
Table S1. Summary of the characterization data for all PDMAC$_x$-PDAAM$_y$ compositions.

Entry	PDMAC DP	Target DAAM DP	Conv. %^{a}	Actual DAAM DP	Theo. M$_n$^{b}	GPC M$_n$^{c}	M$_w$/M$_n$^{c}	DLS Diameter / nm (PdI)^d	Assigned morphology^e
1	40	50	100	50	12800	8900	1.13	144 (0.62)	S+W
2	40	70	100	70	16200	10800	1.24	125 (0.56)	S+W
3	40	85	100	85	18700	12700	1.20	352 (0.55)	S+W
4	40	90	100	90	19600	14800	1.27	-	S+W
5	40	95	100	95	20400	14900	1.25	-	S+W
6	40	100	99	99	21100	14000	1.28	403 (0.45)	W
7	40	105	100	105	22100	16200	1.26	-	W+V
8	40	110	100	110	22900	16900	1.30	-	W+V
9	40	115	100	115	23800	17000	1.30	-	W+V
10	40	120	100	120	24600	16300	1.22	432 (0.27)	W+V
11	40	140	100	140	28000	18600	1.20	467 (0.23)	V
12	40	150	100	150	29700	18200	1.38	560 (0.25)	V
13	40	200	99	198	37800	23700	1.43	559 (0.16)	V
14	46	54	100	54	14000	10600	1.14	41 (0.23)	S+W
15	46	65	100	65	15900	11800	1.15	49 (0.16)	S+W
16	46	76	100	76	17800	13000	1.16	95 (0.19)	S+W
17	46	87	100	87	19600	14100	1.27	127 (0.40)	S+W
18	46	98	100	98	21500	15200	1.20	188 (0.37)	W+V
19	46	109	100	109	23400	16400	1.20	168 (0.19)	W+V
20	46	131	100	131	27000	19100	1.22	332 (0.20)	W+V
21	46	176	98	172	34000	23100	1.27	452 (0.17)	V
22	46	218	99	216	41500	28900	1.27	453 (0.16)	V
23	58	57	100	57	15800	9700	1.27	31 (0.04)	S+W
24	58	69	100	69	17800	10900	1.28	37 (0.05)	S+W
25	58	80	100	80	19700	12000	1.30	48 (0.08)	S+W
26	58	92	99	91	21500	14600	1.28	75 (0.16)	S+W
27	58	92	100	92	21700	13400	1.33	49 (0.06)	S+W
28	58	103	100	103	23500	14500	1.34	58 (0.09)	S+W
29	58	109	98	107	24200	17200	1.22	95 (0.09)	W+V
30	58	126	100	126	27400	18700	1.30	81 (0.09)	W+V
31	58	138	100	138	29500	20000	1.29	96 (0.05)	W+V
32	58	144	99	143	30300	18000	1.31	96 (0.08)	W+V
33	58	149	100	149	31300	21000	1.30	117 (0.07)	V
34	58	161	100	161	33400	22200	1.33	128 (0.08)	V
35	58	172	99	170	34900	23600	1.39	397 (0.17)	V
36	58	172	100	172	35200	22200	1.33	157 (0.11)	V
37	58	201	100	201	40100	24500	1.38	279 (0.28)	V
38	58	207	100	207	41100	26300	1.38	248 (0.19)	V
39	58	218	100	218	43000	27300	1.37	337 (0.13)	V
40	58	230	98	225	44200	27100	1.54	412 (0.11)	V
41	58	230	99	228	44700	25900	1.37	360 (0.15)	V
42	58	230	100	230	45000	28500	1.37	373 (0.13)	V
43	58	230	100	230	45000	31100	1.39	402 (0.19)	V
44	58	345	99	342	64000	34600	1.44	410 (0.12)	V
45	68	78	100	78	20300	14400	1.21	40 (0.09)	S
46	68	104	100	104	24700	17400	1.24	47 (0.08)	S
47	68	157	100	157	33700	23400	1.32	53 (0.09)	S
48	68	209	99	207	42100	26300	1.56	65 (0.05)	S
49	68	417	99	413	80000	46400	1.68	-	S
50	68	626	99	620	112000	60300	1.80	150 (0.03)	S
51	77	75	100	75	20700	14700	1.21	38 (0.05)	S
52	77	100	100	100	24900	17400	1.25	46 (0.14)	S
53	77	150	99	149	33100	20400	1.41	53 (0.06)	S
54	77	200	99	198	41500	26500	1.47	60 (0.05)	S
55	77	300	99	297	58300	37100	1.52	75 (0.02)	S
56	77	400	99	396	75000	47900	1.53	87 (0.03)	S
57	77	500	99	495	91800	58200	1.57	100 (0.03)	S
58	77	600	98	588	107500	66600	1.56	113 (0.03)	S

^{a} ^{1}H NMR spectroscopy in CD$_3$OD, ^{b} $M_{n,th} = \left(([DAAM]_0/[PDMAC]_0) \times DAAM\ conv \times M_{DAAM} \right) + M_{PDMAC}$, ^{c} Determined by DMF GPC vs. PMMA standards ^{d} Determined by dynamic light scattering on 0.1 % w/v dispersions in pH 2.5 water ^{e} Determined by TEM studies of 0.1 % w/v aqueous dispersions at pH 2.5. S = pure spheres, S+W = mixed phase of spherical micelles and worms, W = pure worms, W+V = mixed phase of worms and vesicles and V = pure vesicles.
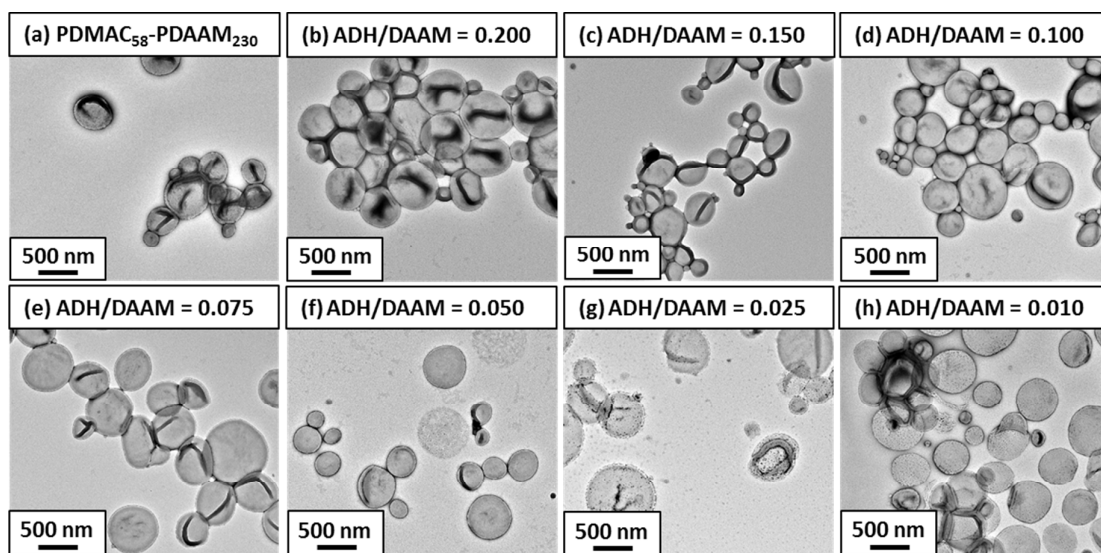
Figure S3. Variation of intensity-average hydrodynamic particle diameter (measured by DLS) and zeta potential with pH recorded at 25 °C for 0.1 % w/w aqueous dispersions of **(a)** a $PDMAC_{58}$-$PDAAM_{91}$ worm/sphere mixed phase **(b)** a $PDMAC_{58}$-$PDAAM_{107}$ worm/vesicle mixed phase **(c)** $PDMAC_{58}$-$PDAAM_{170}$ vesicles **(d)** $PDMAC_{40}$-$PDAAM_{140}$ vesicles **(e)** $PDMAC_{40}$-$PDAAM_{99}$ worms. **(f)** TEM images obtained for a 0.1 % w/w aqueous $PDMAC_{40}$-$PDAAM_{99}$ dispersion at pH 2.5 and pH 9.

Figure S4. Variation of intensity-average hydrodynamic particle diameter and polydispersity (determined by DLS) with temperature on heating a 0.1% w/w aqueous dispersion of (a) $PDMAC_{58}$-$PDAAM_{170}$ vesicles and (b) $PDMAC_{40}$-$PDAAM_{99}$ worms from 4 °C to 50 °C followed by cooling from 50 °C to 25 °C at 5 °C intervals, allowing 15 min for thermal equilibrium at each temperature. (c) TEM images obtained for a 0.1 % w/w aqueous $PDMAC_{40}$-$PDAAM_{99}$ dispersion at 20 °C and 50 °C.

Figure S5. FT-IR spectra recorded for the freeze-dried copolymer products arising from the reaction of a 20 % w/w aqueous dispersion of $PDMAC_{58}$-$PDAAM_{230}$ vesicles with ADH at 25 °C for 6 h using ADH/DAAM molar ratios of 1.00, 0.50, 0.25 or 0.10. The arrow indicates the carbonyl band assigned to the DAAM residues.

Figure S6. TEM images obtained for (a) a 0.1 % w/w *aqueous* dispersion of linear PDMAC$_{58}$-PDAAM$_{230}$ vesicles at pH 2.5 and (b-h) a series of 0.1 % w/w *methanolic* dispersions of PDMAC$_{58}$-PDAAM$_{230}$ vesicles crosslinked using ADH/DAAM molar ratios of 0.200, 0.150, 0.100, 0.075, 0.050, 0.250 or 0.010, respectively.